ACS OMEGA

http://pubs.acs.org/journal/acsodf

Article

Mechanism Study of Imidazole-Type Deep Eutectic Solvents for Efficient Absorption of CO_2

Shengyou Shi, Shuie Li,* and Xiangwei Liu

Cite This: *ACS Omega* 2022, 7, 48272−48281

Read Online

ACCESS | Metrics & More | Article Recommendations

ABSTRACT: Deep eutectic solvents (DESs) are a new class of green solvents that exhibit unique properties in various process applications. In this regard, this study evaluated imidazole-type DESs as solvents for carbon dioxide (CO_2) capture. A series of imidazole-type DESs with different ratios was prepared through one-step synthesis. The absorption capacity of CO_2 in imidazole-type DESs was measured through weighing, and the effects of temperature, hydrogen bond acceptors, hydrogen bond donors, and water content were discussed. DESs absorbed the effects of CO_2. Im-MEA (1:2) was selected to linearly fit $\ln\eta$ and $1/T$ using the Arrhenius equation under variable temperature conditions, and a good linear relationship was found. The results show the best absorption effect for Im-MEA (1:4). At 303.15 K and 0.1 MPa, the absorption capacity of Im-MEA (1:4) was as high as 0.323 g CO_2/g DES; through five times of absorption−desorption after the cycle, the absorption capacity of DES was almost unchanged. Finally, the mechanism of CO_2 absorption was studied using Fourier transform infrared and nuclear magnetic resonance spectroscopy. The absorption mechanism of imidazole-type DESs synthesized using imidazole salt and an amine-based solution was chemical absorption, and the reaction formed carbamate (−NHCOO) to absorb CO_2.

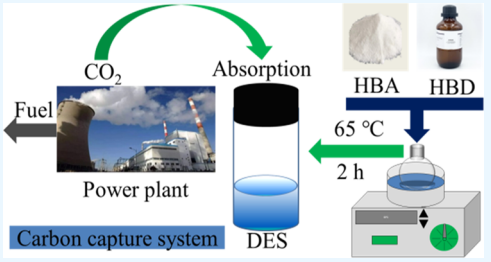

1. INTRODUCTION

Reducing carbon dioxide (CO_2) emissions is key to mitigating climate change. The annual increase in global CO_2 emissions leads to the problem of global climate change, which is one of the most challenging problems for mankind.[1,2] In recent years, CO_2 capture and storage (CCS) technology has been recognized as an effective method for reducing CO_2 emissions.[3] CO_2 capture methods include precombustion capture, oxygen combustion, and postcombustion capture. Postcombustion capture is particularly attractive for addressing climate framework goals, as one can retrofit existing power plants, one of the main sources of anthropogenic CO_2 emissions.[4,5] At present, 25−30 wt % alkanolamine solvent is most widely used in the industry to absorb CO_2. The capture of CO_2 by alkanolamines has the advantages of high absorption, high selectivity, and low cost.[6] Ethanolamine (MEA) can react chemically with acidic CO_2 because of its strong basicity, and its thermal reaction is as high as (~80.0 kJ/mol).[7,8] The reaction product is then decomposed by heating, thereby realizing the recycling of the absorbent. However, the aqueous solution of alkanolamine has inherent defects, such as easy oxidative degradation and high energy consumption for regeneration, which increases the decarbonization cost. Moreover, this method also faces many problems, such as the decomposition of toxic byproducts at high temperatures, the evaporation loss of regenerated alkanolamine, and the corrosion of equipment by alkaline aqueous solution. Thus, finding a green solvent to replace alkanolamine for absorbing CO_2 is particularly important.

In the past few decades, ionic liquid (IL) substitutes for alkanolamine solutions for CO_2 absorption have received great attention. ILs have low saturated vapor pressure, nonvolatile and stable properties, and a controllable structure. Usually, their melting point is lower than 100 °C. At room temperature, they are liquid molten salts composed entirely of anions and cations. The cations are mostly quaternary phosphonium salts and quaternary ammonium salts. In this regard, the deep eutectic solvent (DES) is considered to be a green solvent and can replace traditional organic solvents.[9−11] DES has both the excellent absorption properties of alkanolamines and the outstanding characteristics of ILs and is considered to have the potential to become a new type of CO_2 absorbent. Moreover, DES has already been used as a new type of green solvent in many fields.

DES refers to a two or three-component eutectic mixture with a solidification point significantly lower than the melting point of the pure substances of each component, generally

Received: October 5, 2022
Accepted: November 29, 2022
Published: December 12, 2022

Table 1. Chemical Names and Properties

chemical name	CAS	MW ($g \cdot mol^{-1}$)	purity (%)	supplier
imidazole	288-32-4	68.08	98	Aladdin Pharma Co
4-methylimidazole	822-36-6	82.10	98	Aladdin Pharma Co
ethanolamine	141-43-5	61.08	99	Aladdin Pharma Co
diethanolamine	111-42-2	105.14	99	Aladdin Pharma Co
CO_2	124-38-9	44.01	99.99	Guizhou Sanhe Gas Co., Ltd., China
N_2	7729-37-9	28.00	99.999	Guizhou Sanhe Gas Co., Ltd., China

below −38−150 °C.[12−14] Because of their properties similar to those of ILs, such as low vapor pressure, good stability, and wide liquid range, they are called ILs analogues.[15,16] In addition to the advantages of ILs, many DES production materials are natural from economic and environmental perspectives. It has the advantages of low cost, low toxicity, easy synthesis, no purification, structural tenability, and good biodegradability. DES can be used as a gas separation agent and is a good substitute for ILs. For instance, Li et al.[17] mixed choline chloride (ChCl) and urea (U) at a temperature of 313.2 K and a pressure of 12.5 MPa, and the CO_2 absorption was 0.301 mol/mol. Hsu et al.[18] named the compound synthesized from ChCl and U in a ratio of 1:2 as reline and added MEA to its aqueous solution at a temperature of 313.2 K−353.2 K and a pressure of 900 kPa. The results showed that the solubility of CO_2 was significantly improved when MEA was added. Sze et al.[19] found that the solubility of the ChCl, Gly, and superbase (1,5-diazabicyclo[4.3.0]non-5-ene) ternary DES system at a ratio of 1:2:6 is 2.4 mmol/g, less than those of traditional ILs. Chemat et al.[20] studied a ternary DES system composed of ChCl, Gly, and L-arginine in a molar ratio of 1:2:0.1. When the temperature was 303.15−323.15 K and the pressure was 20 bar, the solubility of CO_2 was 0.242 g/g. Li et al.[17] introduced metal chloride into TMAC-MEA at a ratio of 1:5:0.1 and left it to absorb CO_2 for 1 h at 50 °C. They found that the system's ability to absorb CO_2 increased to 36.81 wt %.

In the current literature, there is little research on imidazole-based DESs for CO_2 absorption, and the most studied are quaternary ammonium salt choline chloride-based DESs. In this study, a series of imidazole-type DES with different proportions were prepared using a one-step synthesis method with imidazoles as hydrogen bond acceptors (HBAs) and alcohol amine solvents as hydrogen bond donors (HBDs). The effects of temperature, HBA, HBD, water content, and other factors on the ability of DES to absorb CO_2 were systematically investigated, and the CO_2 absorption mechanism was studied.

2. EXPERIMENTAL SECTION

2.1. Chemical Names and Properties. The chemical names used in this paper and their characteristics are shown in Table 1 below.

2.2. Analytical Testing Instruments. Thermogravimetric analyzer (TGA5500, TA Instruments); Brookfield DV-II+Pro viscometer, Brookfield; Thermo Scientific Nicolet iS20 Fourier transform infrared spectroscopy (FTIR), Thermo Fisher Scientific; Bruker 600M nuclear magnetic resonance spectrometer (NMR), Nippon Electronics Co., Ltd.; Electronic Balance, AR224CN, accuracy of $\pm 2 \times 10^{-4}$ g, Ohaus Instrument Co., Ltd.; Trace Moisture analyzer, WS-2A; and Shandong Zibo three-pump, Cosen Instrument Ltd (Figure 1).

2.3. Preparation of DESs. Alm/BMEA (lm-MEA) and Alm/BDEA (lm-DEA) were prepared by mixing imidazole and

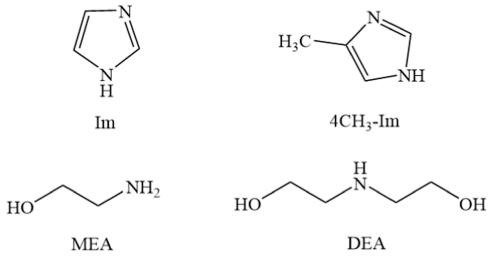

Figure 1. Molecular formulas of HBAs and HBDs.

4-methylimidazole as HBAs with ethanolamine and diethanolamine as HBDs at a given molar ratio, A4CH_3-lm/BMEA (4CH_3-lm-MEA) and A4CH_3-lm/BDEA (4CH_3-lm-DEA), where *A* and *B* represent moles (*A* = 1, *B* = 2, 3, and 4). In practice, the mixture was heated and stirred at 65 °C until a homogeneous liquid was formed. Subsequently, the resulting DES was cooled to room temperature and left for 24 h to ensure that no crystal formation occurred. The melting points of the prepared lm-MEA DES with different ratios are shown in Figure 2. The figure shows that the melting points of DESs

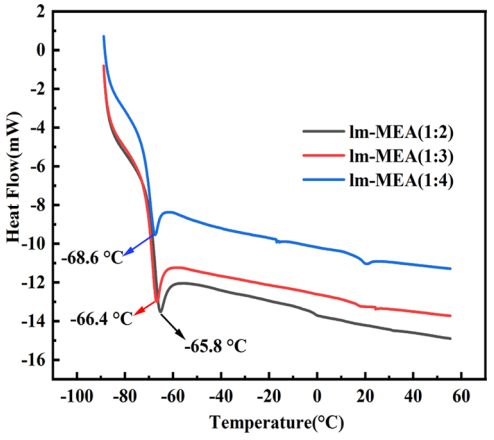

Figure 2. Melting point of DESs.

are significantly lower than that of each raw material component, which proves the formation of deep eutectic solvents. The CO_2 absorption capacity is calculated gravimetrically. The water content of each DES was measured using a micro moisture analyzer before use, and the results were all less than 0.1% (mass fraction). The accuracy of the electronic balance was ±0.1 mg. The molecular structures of the HBAs and HBDs used in this study are shown in Figure 1.

2.4. Experiment Content. *2.4.1. Determination of Viscosity.* Im-MEA (1:2), Im-MEA (1:3), and Im-MEA (1:4) were chosen for measuring viscosity at 30−60 °C. Each sample was tested three times at the same temperature, and the average value was taken as the sample viscosity value.

https://doi.org/10.1021/acsomega.2c06437
ACS Omega 2022, 7, 48272−48281

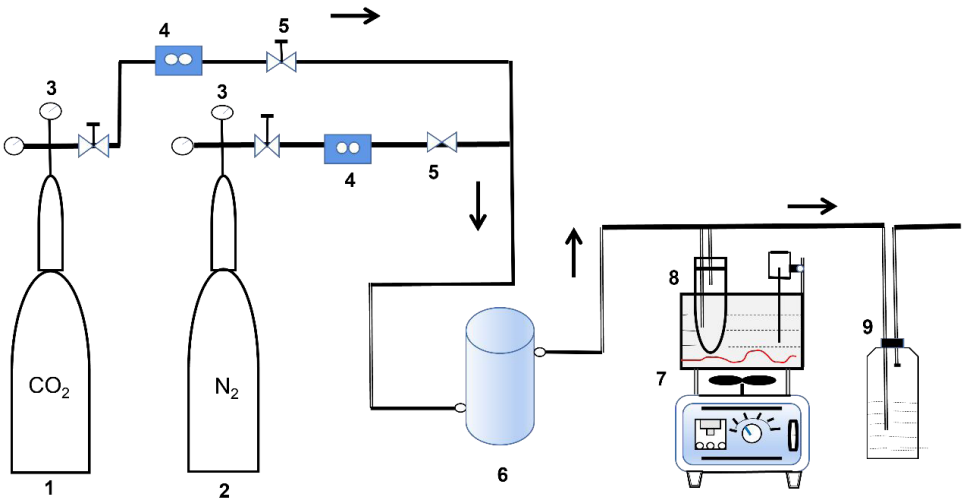

1. CO_2
2. N_2
3. pressure reducing valve
4. gas flowmeter
5. Valve
6. gas buffer chamber
7. constant temperature water bath pot
8. absorption tube
9. NaOH solution

Figure 3. CO_2 absorption device.

2.4.2. Determination of Stability. The samples were analyzed using a thermogravimetric analyzer and N_2 as an inert gas. The heating rate was 10 °C/min, and the temperature range was 0−500 °C.

2.4.3. CO_2 Absorption. The CO_2 absorption capacity is calculated by the gravimetric method, and the calculation formula is as follows[21]

$$\alpha = \frac{m_{CO_2}}{m}$$

where m represents the total mass of the absorbent (g) and m_{CO_2} is the mass of CO_2 absorbed (g). Figure 3 below shows a diagram of a CO_2 absorption device.

2.4.4. Desorption of CO_2. CO_2 was desorbed under the conditions of heating and purging with N_2. The saturated absorbent was added into the desorption bottle, which was then placed in a constant temperature water bath at 80 °C. Then, the inlet of the desorption bottle was connected to N_2. The CO_2 release was monitored by weighing the mass change during the desorption process. When the weight of the test tube did not change, the desorption was considered complete. During the entire absorption and desorption weighing process, a clean paper towel was used for wiping to ensure that there was no residual water from the water bath. The method to quantify the solvent loss in desorption experiments is

$$\chi = \frac{n_{regeneration}}{n}$$

where χ represents the regeneration efficiency (%); $n_{regeneration}$ represents the mass absorption capacity (g CO_2/g DES) of the absorbent after regeneration; and n represents the absorption capacity of the fresh absorbent (g CO_2/g DES).

Table 2 shows the experimental factors and numerical range.

Table 2. Experimental Factors and the Numerical Range

no	factors	value
1	mol ratio	1:2, 1:3, 1:4, 3:2
2	temperature (°C)	30, 40, 50, 60
3	water content (% vol)	0, 10, 20
4	gas velocity (mL/min)	40, 60, 80

3. RESULTS AND DISCUSSION

3.1. Effects of the HBD to HBA Molar Ratio on CO_2 Absorption by DES. A series of imidazole-type DES synthesized in experiments were studied to explore the optimal molar ratio of CO_2 absorption by DES, and the absorption was conducted under certain experimental conditions. The CO_2 absorption curves of several DESs are shown in Figure 4.

Figure 4 shows that selecting different HBDs, HBAs, or amount ratios of the two substances has an impact on the absorption of CO_2. For different absorption systems, the influencing factors are also different. Under the same ratio, when the HBD was MEA or DEA and the HBA was Im or $4CH_3$-Im, the CO_2 absorption capacity of DES was Im-MEA (1:4) > $4CH_3$-Im-MEA (1:4) > $4CH_3$-Im-DEA (1:4) > Im-DEA (1:4) > Im-MEA (3:2) > Im-DEA (3:2). Because the viscosity of DEA was greater than that of MEA, it was formed with HBD as DEA. The amount of CO_2 absorbed by DES was less than that of DES formed with HBD as MEA, which was reasonable. It can be seen from the above that the comprehensive performance of DES can be regulated by changing different HBDs and HBAs or changing the amount ratio of the two substances. From Figure 4d, the absorption capacity of CO_2 increased with the increase in the molar ratio of HBD. Among DES synthesized above, Im-MEA (1:4) had the best absorption capacity for CO_2, reaching 0.323 g CO_2/g DES. Thus, the following research is mainly based on the Im-MEA system.

3.2. Viscosity of DESs. Viscosity is a basic parameter related to the determination of absorbent properties and equipment design and selection.[22] Figure 5a shows the viscosity diagram of three different molar ratios of DESs: Im-MEA (1:2), Im-MEA (1:3), and Im-MEA (1:4). The viscosity decreased with increasing temperature. In addition, we also

https://doi.org/10.1021/acsomega.2c06437
ACS Omega 2022, 7, 48272−48281

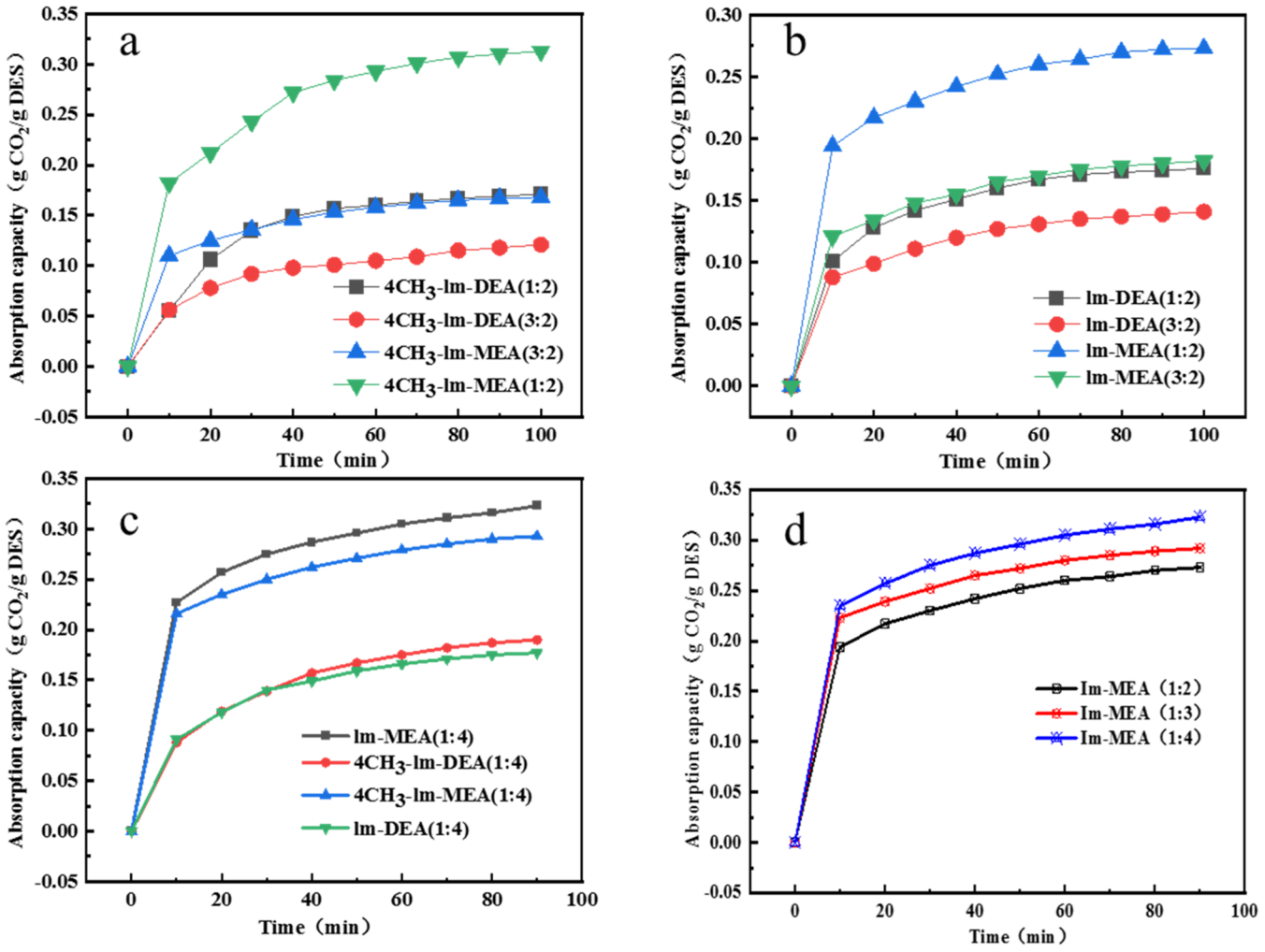

Figure 4. (a,b) HBAs $4CH_3$-Im and Im and mole ratios of different HBDs. (c) Different mole ratios of the same HBAs. (d) Different molar ratios of the same DESs.

studied the relationship between the viscosity and temperature of lm-MEA (1:2) DES between 30 and 60 °C and found that the relationship between viscosity and temperature followed the Arrhenius equation[23]

$$\ln \eta = \ln A + E\eta/(RT)$$

where η is the viscosity of DES (mPa·s); A denotes the viscosity parameter; $E\eta$ is the flow activation energy (kJ/mol); R is the molar gas constant; and T is the thermodynamic temperature (K).

The relationship of In n to $1/T$ for DES is shown in Figure 5b. $E\eta$ has a good linear relationship with $1/T$, and it increases with the decrease in temperature. The calculated values of A and $E\eta$ from the intercept and slope were 1.75×10^{-7} and −28.6 kJ/mol, respectively, and the linear correlation coefficient R^2 was 0.9967.

We also studied the viscosity change of DES during CO_2 absorption. Figure 5c shows the viscosity changes of Im-MEA DES systems with different molar ratios before and after CO_2 gas absorption within 90 min at 30 °C and 1 bar. Obviously, after the absorption of CO_2 gas, the viscosity of DES increased greatly. Before the absorption of CO_2, the viscosity values of the three DES are relatively close. After 90 min of CO_2 gas, the viscosity of Im-MEA (1:2), Im-MEA (1:3), and Im-MEA (1:4) increased significantly. For example, the viscosity of Im-MEA (1:3) and Im-MEA (1:4) increased 27.4 times (from 15.2 to 416.3 mPa·s) and 28.8 times (from 14.9 to 429.5 mPa·s), respectively. After CO_2 absorption, the viscosity value of Im-MEA (1:2) was 391.5 mPa·s, and the increase of viscosity after CO_2 absorption was positively correlated with the absorption capacity. The reason for this result may be related to the absorption capacity of DES for CO_2 gas. Therefore, the increase in the viscosity value was also the smallest, and the entry of CO_2 will lead to an increase in viscosity of the DES system.

3.3. Thermal Stability of DESs. Thermal stability is an important indicator for measuring the practical applications of gas absorbents, and high thermal stability is conducive to the recycling of absorbents and[24,25] reducing use costs and secondary pollution. Figure 6a is a thermogravimetric diagram, whereas Figure 6b−d, respectively, represents the three different molar ratios of Im-MEA (1:2), Im-MEA (1:3), and Im-MEA (1:4).

The thermal stability results show that the weight loss of the sample started from about 327.15 K, and it decomposed completely at about 553.15 K. Thereafter, the mass of the sample had no obvious change with the increase in temperature. The 5% mass loss temperatures T (d, 5%) of the samples were 359.15, 360.15, and 361.15 K, respectively, showing good thermal stability. Meanwhile, the initial

https://doi.org/10.1021/acsomega.2c06437
ACS Omega 2022, 7, 48272−48281

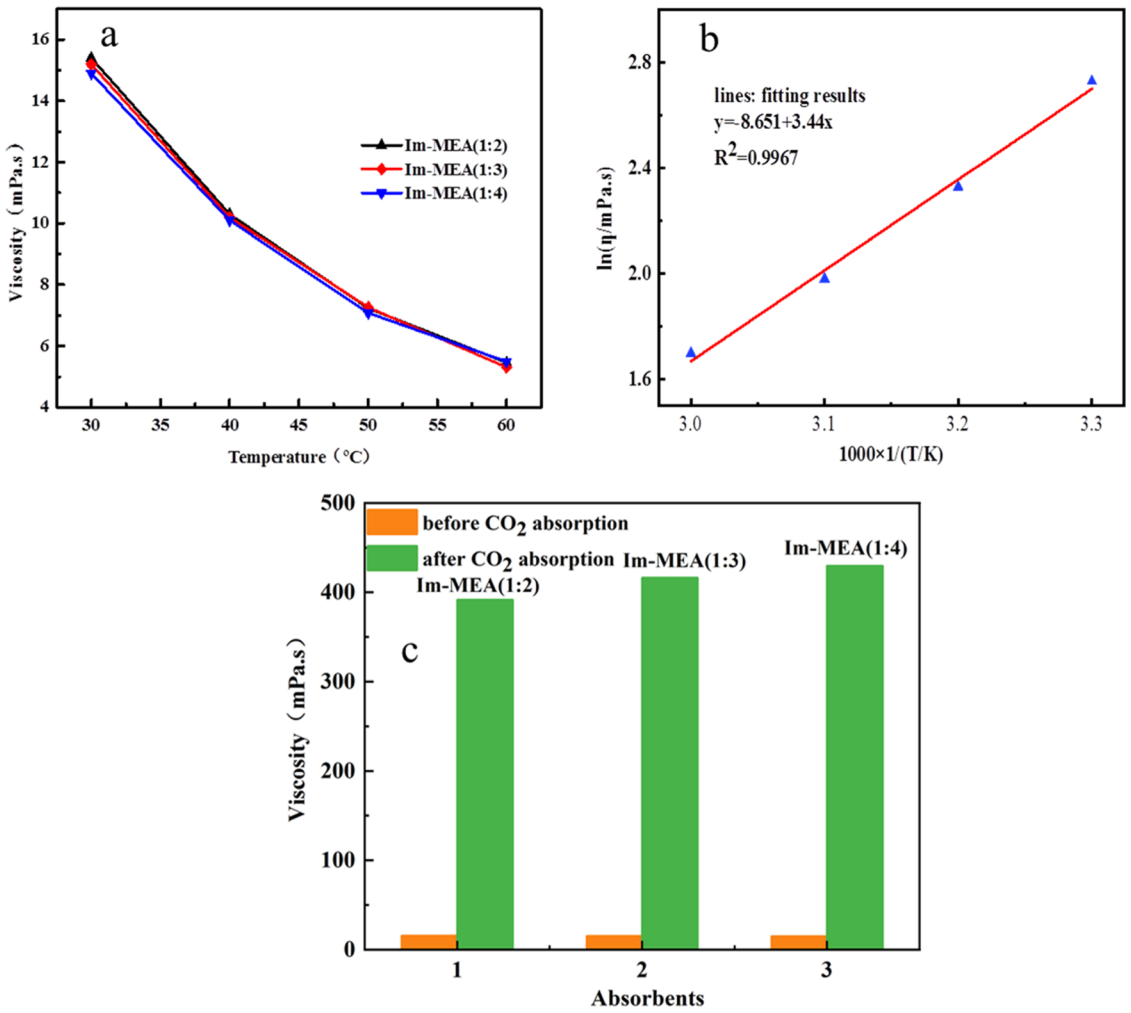

Figure 5. (a) Changes of the viscosity of three DESs with temperature. (b) Fitting diagram of three kinds of Im-MEA (1:2) DESs. (c) Viscosity of DESs before and after CO_2 absorption.

decomposition temperature of Im-MEA (1:4) was 361.15 K and its stability was higher than the former two samples. The main reason for this high stability was the hydrogen bond interaction between HBA and HBD resulting in a complex hydrogen bond network. The thermogravimetric loss of Im-MEA (1:4) DES is under 343.15 K, and the N_2 purge condition is shown in Figure 6a. The weight loss values for Im-MEA (1:4) DES were 0.05 and 0.42%, respectively, over a longer period (2 h). Therefore, the thermal stability of the current DES under absorption and desorption conditions is acceptable.

3.4. Effects of Temperature on CO_2 Absorption by DESs. The CO_2 absorption capacity of Im-MEA (1:4) was tested under different temperature conditions, and the experimental results are shown in Figure 7.

Figure 7 shows that the absorption capacity of acid gas CO_2 in Im-MEA (1:4) decreased significantly with the gradual increase in temperature. For example, when the temperature increased from 303.15 to 333.15 K, the absorption capacity of Im-MEA (1:4) decreased from 0.323 to 0.294 g CO_2/g DES, respectively. This indicates that low temperatures facilitate easy absorption, whereas high temperatures facilitate easy desorption. Moreover, the heating of the saturated absorbent can desorb CO_2 gas and realize absorption regeneration and recycling of chemicals. DES is beneficial to applications in industrial decarbonization.

3.5. Comparison of CO_2 Absorption by DESs. The absorption capacity of the studied DES was compared with those of other DESs reported in the literature to evaluate the CO_2 absorption performance of DES in this study, and the results are listed in Table 3.

As shown in Table 3, the absorption capacity of CO_2 in this experiment is compared with the data in the literature. The study shows that the absorption capacity of Im-based DESs for CO_2 is better, which ranged from 0.193 to 0.323 g CO_2/g DES. The absorption capacity of CO_2 in Im-MEA (1:4) is higher than those of common DESs [e.g., [TETA]Cl-thymol (1:3), [P_{2222}][Triz]-EG(1:2), [TETA]Cl-EG(1:3), and [HDBU][Triz]-EG(7:3)], but lower than that of [MEA]-[Cl]-EDA (1:3) DES. This is because ethylenediamine (EDA) contains one more NH_2 than MEA, which is beneficial for absorbing CO_2 through the formation of hydrogen bonds. Compared with DESs reported in the literature, Im-based DESs have greater advantages in the synthesis process and raw material costs and are worthy of further research.

3.6. Influence of Water Content on CO_2 Absorption by DESs. The increase in viscosity reduced the mass transfer of CO_2 in DES and the migration of free electrons, resulting in a decrease in the absorption rate of CO_2. Meanwhile, the

https://doi.org/10.1021/acsomega.2c06437
ACS Omega 2022, 7, 48272−48281

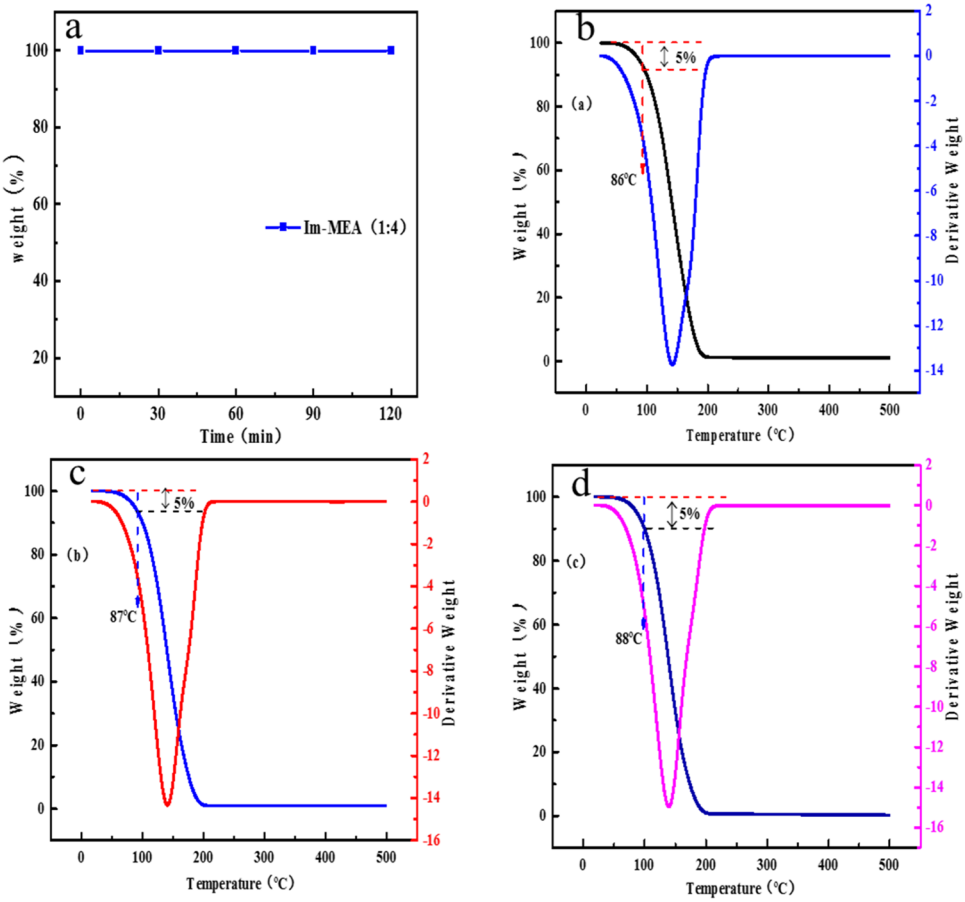

Figure 6. (a) Thermogravimetric diagram of Im-MEA (1:4) DESs at 343.15 K under N_2 purging. (b−d) TGA curves of three Im-MEA DESs with different ratios.

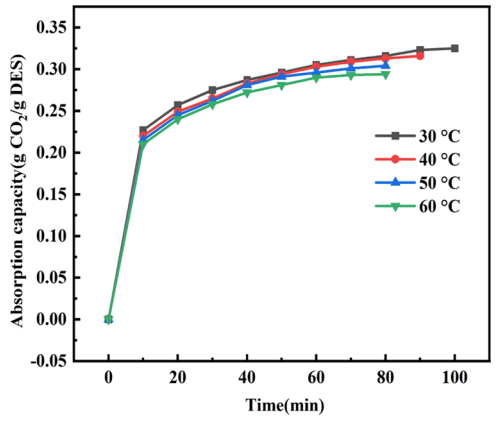

Figure 7. CO_2 absorption capacity of Im-MEA (1:4) at different temperatures.

increase in water content reduced the viscosity of DES and reduced the mass transfer rate of CO_2.[37] Water can also form hydrogen bonds with DES to reduce the effect of intramolecular hydrogen bonds in DES, thereby increasing the free volume of DES and enhancing the CO_2 capture ability.[26,30,38] This section investigates the effect of water content on CO_2 uptake by lm-MEA (1:4), $4CH_3$-lm-MEA (1:4), lm-DEA (1:4), and $4CH_3$-lm-DEA (1:4). The results are shown in Figure 8a−c.

Figure 8 shows that with the increase in water content, the effect of DES on CO_2 absorption became more obvious. This

Table 3. Comparison of the CO_2 Absorption Capacity of DES with Those of DESs in the Literature

absorbents	T (°C)	P (kPa)	CO_2 absorption capacity (g CO_2/g DES)	refs
Im-MEA (1:4)	30	100	0.323	this work
Im-DEA (1:4)	30	100	0.181	this work
$4CH_3$-Im-MEA (1:4)	30	100	0.297	this work
$4CH_3$-Im-DEA (1:4)	30	100	0.193	this work
DBN-EU (2:1)	45	100	0.299	26
DBN-BmimCl-Im (1:1:1)	25	100	0.367	27
[TETA]Cl-thymol (1:3)	40	100	0.090	28
[P_{2222}][Triz]-EG (1:2)	25	100	0.106	29
[MEA][Cl]-EDA (1:3)	30	100	0.337	30
[TETA]Cl-EG (1:3)	40	100	0.175	31
[HDBU][Triz]-EG (7:3)	40	100	0.106	32
ChCl-MEA (1:6)	30	100	0.290	33
ChCl-DEA (1:6)	30	100	0.150	33
0.44PEI	30	101	1.690[a]	34
0.30PEI + 0.18[emim][Ac]	30	101	1.220[a]	34
PEHA/CDMAC	25	101	1.310[a]	35
PEHA/CDMAC	100	101	0.210[a]	35
[emim][Gly] + [emim][Ac]	25	101	2.980[b]	36
[emim][Ala] + [emim][Ac]	40	101	2.050[b]	36

[a]Capacity in mmol CO_2/g adsorbent. [b]Capacity in mol/kg.

https://doi.org/10.1021/acsomega.2c06437
ACS Omega 2022, 7, 48272−48281

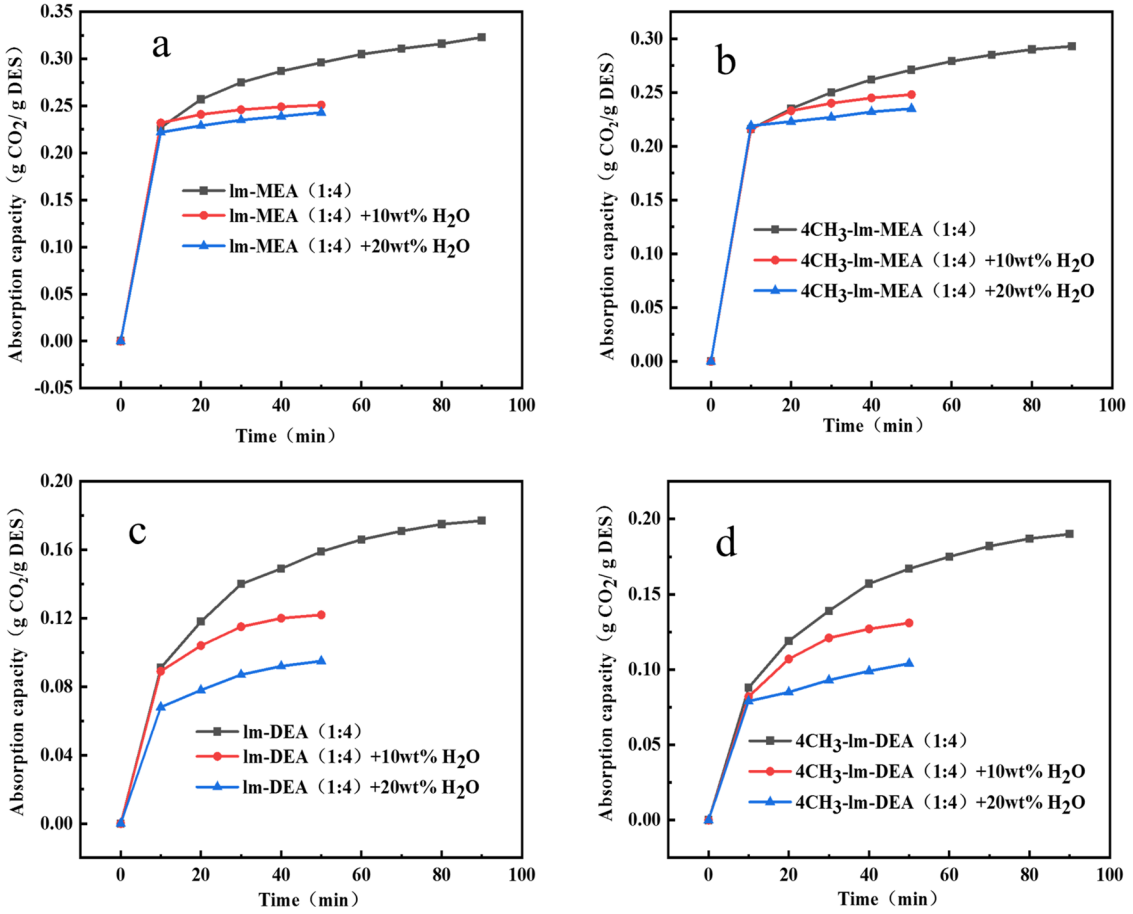

Figure 8. (a–d) Water content of different DES systems.

was because the addition of too much water reduced the concentration of the effective solvent DES, destroyed the hydrogen bond network, and led to a decrease in the absorption capacity of DES. Therefore, the presence of water has a great inhibitory effect on CO_2 absorption for DES-containing primary and secondary amines. In addition, in this study, the reaction product of DES and CO_2 was carbamate, and excess water in the system would react with carbamate to generate carbonic acid, which decomposed into water and CO_2.[39] This resulted in a decrease in the ability of DES to absorb CO_2.

3.7. Cycling Performance of Im-MEA (1:4). The reusability of the absorbent has an important impact on the operating cost of the absorption process and can reduce the generation of pollutants. Thus, the recycling performance of Im-MEA (1:4) was studied in this paper, and the results are shown in Figure 9.

Figure 9 shows that after five cycles of DES absorption–desorption, the CO_2 absorption capacity of DES can still reach 0.315 g CO_2/g DES, compared with the CO_2 absorption capacity (0.323 g CO_2/g DES) in the initial absorption process. There was thus no major change, indicating that the absorbent had better circulation; however, this was only for five cycles. After DES was regenerated, the captured CO_2 was not completely released, and its CO_2 absorption slightly decreased. This was because the carbamate generated by the chemical reaction between DES and CO_2 was relatively stable, and it did not easily completely decompose during regeneration. Thus, a little part of CO_2 remained in DES.

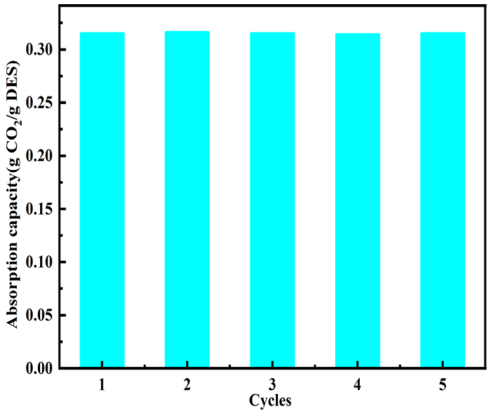

Figure 9. Im-MEA (1:4) DES absorption cycle diagram after five cycles.

3.8. Mechanism Analysis of CO_2 Absorption by DES. The interaction of Im-MEA (1:4) with CO_2 was investigated using NMR. The NMR spectra of Im-MEA (1:4) before and after CO_2 absorption are shown in Figure 10.

The ^{1}H NMR results confirm the conversion of the $-CH_2-NH_2$ group to $-CH_2-NH$, consistent with the new peaks at chemical shifts 2.97 and 2.73 ppm, and other peaks with the chemistry of ^{1}H NMR before CO_2 absorption displacement confirmed the agreement. After the absorption of CO_2, a new peak appeared at the chemical shift of 5.94 ppm, which was due to the protonation of NH on the imidazole ring to form NH_2. ^{13}C NMR shows that two new peaks appeared after CO_2

https://doi.org/10.1021/acsomega.2c06437
ACS Omega 2022, 7, 48272–48281

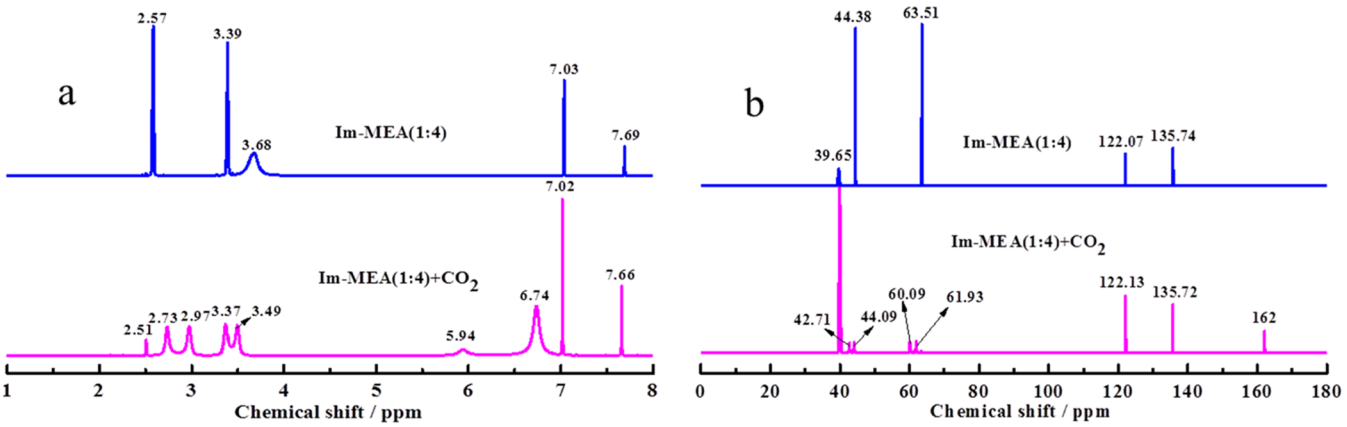

Figure 10. (a) ^{1}H NMR before and after CO_2 absorption by Im-MEA (1:4) and (b) ^{13}C NMR before and after CO_2 absorption by Im-MEA (1:4).

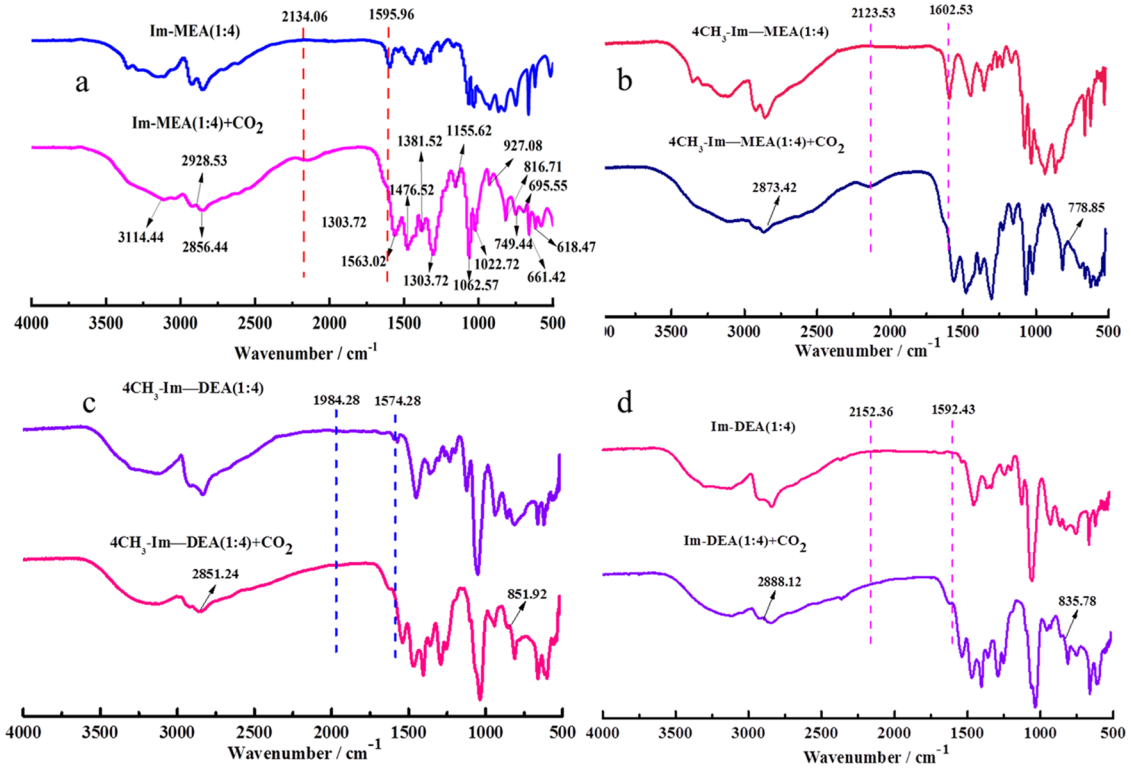

Figure 11. (a–d) Infrared spectra of different DES systems before and after CO_2 absorption.

absorption,162 ppm from the carbon peak on carbamate (−NHCOO) and 42.71 ppm from carbon on $-CH_2-NH$, that is, −NHCOO is formed, consistent with the literature.[40,41] The peak at 41.25 ppm was due to the formation of −NHCOO resulting in the splitting of $-CH_2$. We further investigated the interaction between CO_2 and DES using FTIR to further prove that the generated species is −NHCOO. Figure 11 characterizes the infrared spectra of DES before and after CO_2 absorption.

For Im-MEA (1:4), there were peaks at 2856.44, 1022.72, and 1062.57 cm^{-1}, and the peak of the −NH primary amine extension at 2856.44 cm^{-1} was weakened after CO_2 absorption.[42] It was proven that −NHCOO was formed between Im-MEA (1:4) and CO_2; thus, the peak at 2856.44 cm^{-1} was weakened. The peak at 1022.72 cm^{-1} represents −C−N stretching, whereas the peak at 1062.57 cm^{-1} represents −C−O stretching.[43] After Im-MEA (1:4) absorbed CO_2, the peaks at 1022.72 and 1062.57 cm^{-1} were both stronger than those during absorption, which also shows that −NHCOO formed between DES and CO_2 at 1022.72 and 1062.57 cm^{-1}. The peak intensity at 1062.57 cm^{-1} was enhanced. Comparing the infrared spectra of Im-MEA (1:4) before and after absorption, it can be seen that after CO_2 absorption, new peaks appeared at 1600−1900 and 816.71 cm^{-1}. A peak at 1600−1900 cm^{-1} corresponds to symmetrically stretched −COO, whereas that at 816.71 cm^{-1} corresponds to −COO bending. The appearance of new peaks at 1600−1900 and 816.71 cm^{-1} and the enhancement of the peaks at 1022.72 and 1062.57 cm^{-1} indicate that −NHCOO was formed after Im-MEA (1:4) absorbed CO_2. The reaction mechanism of DES and CO_2 was confirmed, and similar phenomena appeared in the b, c, and d diagrams.

It has been reported that MEA and DEA can react directly with CO_2 to form carbamates in two steps.[44]

https://doi.org/10.1021/acsomega.2c06437
ACS Omega 2022, 7, 48272−48281

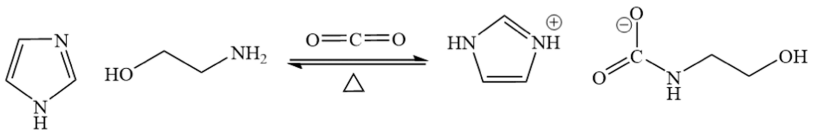

Figure 12. Possible mechanism of CO_2 absorption by Im-MEA DES.

First step:

$$CO_2 + R_1R_2NH \Leftrightarrow R_1R_2NHCOOH$$

Second step:

$$R_1R_2NHCOOH + R_1R_2NH \Leftrightarrow R_1R_2NHCOO^- + R_1R_2NH_2^+$$

Figure 12 shows the possible mechanism of CO_2 absorption by Im-MEA DES.

4. CONCLUSIONS

This study examined the use of imidazole-type DES in CO_2 capture applications. Different proportions of DES were designed to improve the CO_2 absorption capacity, and they all showed good CO_2 absorption capacities. The physical properties and absorption performance of the Im-MEA DES system were measured. The results show that its thermal stability is good, and Im-MEA (1:4) has the best absorption performance. The viscosity of the Im-MEA DES system was measured, and viscosity was linearly fitted under variable temperature conditions, showing a good linear correlation. We also systematically studied the effects of different HBAs, HBDs, temperatures, and different water contents on the absorption of CO_2 by DES. Changing the ratio of HBAs, HBDs, and their substances can regulate the comprehensive performance of DES. Temperature and water content affected the absorption of CO_2 by DES. At 30 °C, the absorption capacity of Im-MEA (1:4) for CO_2 was 0.323 g CO_2/g DES and Im-MEA (1:4) DES showed good recycling performance after five absorption−desorption cycles. Thereafter, the absorption performance remained basically unchanged. The analysis results of FTIR and NMR spectra showed that the absorption of CO_2 by Im-MEA (1:4) was through chemical absorption, and CO_2 reacted with $-NH_2$ of MEA to form −NHCOO. This study demonstrated that imidazole-type DES is an excellent, inexpensive, and simple solvent for CO_2 capture.

AUTHOR INFORMATION

Corresponding Author

Shuie Li − *Key Laboratory of Metallurgical Engineering and Process of Energy Saving of Guizhou Province, College of Materials and Metallurgy, Guizhou University, Guiyang 550025, P. R. China;* orcid.org/0000-0002-6070-0063; Email: 568144269@qq.com

Authors

Shengyou Shi − *Key Laboratory of Metallurgical Engineering and Process of Energy Saving of Guizhou Province, College of Materials and Metallurgy, Guizhou University, Guiyang 550025, P. R. China*

Xiangwei Liu − *Key Laboratory of Metallurgical Engineering and Process of Energy Saving of Guizhou Province, College of Materials and Metallurgy, Guizhou University, Guiyang 550025, P. R. China*

Complete contact information is available at: https://pubs.acs.org/10.1021/acsomega.2c06437

Notes

The authors declare no competing financial interest.

ACKNOWLEDGMENTS

This work was financially supported by the Science and Technology Department of Guizhou Province in China (project number: QKHZC [2019] 2164).

REFERENCES

(1) Li, Z.; Wang, L.; Li, C.; Cui, Y.; Li, S.; Yang, G.; Shen, Y. M. Absorption of carbon dioxide using ethanolamine-based deep eutectic solvents. *ACS Sustainable Chem. Eng.* **2019**, *7*, 10403−10414.

(2) Wu, X.; Fan, X.; Xie, S.; Lin, J.; Cheng, J.; Zhang, Q.; Chen, L.; Wang, Y. Solar energy-driven lignin-first approach to full utilization of lignocellulosic biomass under mild conditions. *Nat. Catal.* **2018**, *1*, 772−780.

(3) Wang, Q.; Luo, J.; Zhong, Z.; Borgna, A. CO_2 capture by solid adsorbents and their applications: current status and new trends. *Energy Environ. Sci.* **2011**, *4*, 42−55.

(4) Leclaire, J.; Heldebrant, D. J. A call to (green) arms: a rallying cry for green chemistry and engineering for CO_2 capture, utilisation and storage. *Green Chem.* **2018**, *20*, 5058−5081.

(5) Nematollahi, M. H.; Carvalho, P. J. Green solvents for CO_2 capture. *Curr. Opin. Green Sustainable Chem.* **2019**, *18*, 25−30.

(6) Rochelle, G. T. Amine scrubbing for CO_2 capture. *Sci.* **2009**, *325*, 1652−1654.

(7) Kim, I.; Svendsen, H. F. Heat of absorption of carbon dioxide (CO_2) in monoethanolamine (MEA) and 2-(aminoethyl) ethanolamine (AEEA) solutions. *Ind. Eng. Chem. Res.* **2007**, *46*, 5803−5809.

(8) McCann, N.; Maeder, M.; Attalla, M. Simulation of enthalpy and capacity of CO_2 absorption by aqueous amine systems. *Ind. Eng. Chem. Res.* **2008**, *47*, 2002−2009.

(9) Taheri, M.; Zhu, R.; Yu, G.; Lei, Z. Ionic liquid screening for CO_2 capture and H_2S removal from gases: The syngas purification case. *Chem. Eng. Sci.* **2021**, *230*, No. 116199.

(10) Taheri, M.; Dai, C.; Lei, Z. CO_2 capture by methanol, ionic liquid, and their binary mixtures: Experiments, modeling, and process simulation. *AIChE J.* **2018**, *64*, 2168−2180.

(11) Lei, Z.; Dai, C.; Wang, W.; Chen, B. UNIFAC model for ionic liquid-CO_2 systems. *AIChE J.* **2014**, *60*, 716−729.

(12) Abbott, A. P.; Capper, G.; Davies, D. L.; Rasheed, R. K.; Tambyrajah, V. Novel solvent properties of choline chloride/urea mixtures. *Chem. Commun.* **2003**, *1*, 70−71.

(13) Adi Kurnia, K.; Zunita, M.; Coutinho, J. A.; Wenten, I. G.; Santoso, D. Development of quantitative structure-property relationship to predict the viscosity of deep eutectic solvent for CO_2 capture using molecular descriptor. *J. Mol. Liq.* **2022**, *347*, No. 118239.

(14) Rozas, S.; Atilhan, M.; Aparicio, S. Bulk liquid phase and interfacial behavior of cineole−Based deep eutectic solvents with regard to carbon dioxide. *J. Mol. Liq.* **2022**, *353*, No. 118748.

(15) Wagle, D. V.; Zhao, H.; Baker, G. A. Deep eutectic solvents: sustainable media for nanoscale and functional materials. *Acc. Chem. Res.* **2014**, *47*, 2299−2308.

(16) Smith, E. L.; Abbott, A. P.; Ryder, K. S. Deep eutectic solvents (DESs) and their applications. *Chem. Rev.* **2014**, *114*, 11060−11082.

(17) Li, X.; Hou, M.; Zhang, Z.; Han, B.; Yang, G.; Wang, X.; Zou, L. Absorption of CO_2 by ionic liquid/polyethylene glycol mixture and the thermodynamic parameters. *Green Chem.* **2008**, *10*, 879−884.

(18) Hsu, Y. H.; Leron, R. B.; Li, M. H. Solubility of carbon dioxide in aqueous mixtures of (reline+monoethanolamine) at T = (313.2 to 353.2) K. *J. Chem. Thermodyn.* **2014**, *72*, 94−99.
(19) Sze, L. L.; Pandey, S.; Ravula, S.; Pandey, S.; Zhao, H.; Baker, G. A.; Baker, S. N. Ternary deep eutectic solvents tasked for carbon dioxide capture. *ACS Sustainable Chem. Eng.* **2014**, *2*, 2117−2123.
(20) Chemat, F.; Gnanasundaram, N.; Shariff, A. M.; Murugesan, T. Effect of L-arginine on solubility of CO_2 in choline chloride+glycerol based deep eutectic solvents. *Procedia Eng.* **2016**, *148*, 236−242.
(21) Liu, X.; Gao, B.; Jiang, Y.; Ai, N.; Deng, D. Solubilities and thermodynamic properties of carbon dioxide in guaiacol-based deep eutectic solvents. *J. Chem. Eng. Data* **2017**, *62*, 1448−1455.
(22) Zhu, J.; Xu, Y.; Feng, X.; Zhu, X. A detailed study of physicochemical properties and microstructure of EmimCl-EG deep eutectic solvents: their influence on SO_2 absorption behavior. *J. Ind. Eng. Chem.* **2018**, *67*, 148−155.
(23) Abbott, A. P.; Harris, R. C.; Ryder, K. S.; D'Agostino, C.; Gladden, L. F.; Mantle, M. D. Glycerol eutectics as sustainable solvent systems. *Green Chem.* **2011**, *13*, 82−90.
(24) Chai, M.; Zhao, W.; Li, G.; Xu, S.; Jia, Q.; Chen, Y. Novel SO_2 phase-change absorbent: mixture of N, N-dimethylaniline and liquid paraffin. *Ind. Eng. Chem. Res.* **2018**, *57*, 12502−12510.
(25) Han, G.; Jiang, Y.; Deng, D.; Ai, N. Solubilities and thermodynamic properties of SO_2 in five biobased solvents. *Chem. Thermodyn.* **2016**, *92*, 207−213.
(26) Jiang, B.; Ma, J.; Yang, N.; Huang, Z.; Zhang, N.; Tantai, X.; Sun, Y.; Zhang, L. Superbase/acylamido-based deep eutectic solvents for multiple-site efficient CO_2 absorption. *Energy Fuels* **2019**, *33*, 7569−7577.
(27) Zhang, N.; Huang, Z.; Zhang, H.; Ma, J.; Jiang, B.; Zhang, L. Highly Efficient and Reversible CO_2 Capture by Task-Specific Deep Eutectic Solvents. *Ind. Eng. Chem. Res.* **2019**, *58*, 13321−13329.
(28) Gu, Y.; Hou, Y.; Ren, S.; Sun, Y.; Wu, W. Hydrophobic Functional Deep Eutectic Solvents Used for Efficient and Reversible Capture of CO_2. *ACS Omega* **2020**, *5*, 6809−6816.
(29) Cui, G.; Lv, M.; Yang, D. Efficient CO_2 absorption by azolide-based deep eutectic solvents. *Chem. Commun.* **2019**, *55*, 1426−1429.
(30) Bi, Y.; Hu, Z.; Lin, X.; Ahmad, N.; Xu, J.; Xu, X. Efficient CO_2 capture by a novel deep eutectic solvent through facile, one-pot synthesis ith lo energy consumption and feasible regeneration. *Sci. Total Environ.* **2020**, *705*, 2−18.
(31) He, J.; Hu, L.; Tang, Y.; Li, H.; Yang, P.; Li, Z. Adsorption features and photocatalytic oxidation performance of $M_{1/3}$ $NbMoO_6$ (M=Fe, Ce) for ethyl mercaptan. *RSC Adv.* **2014**, *4*, 22334−22341.
(32) Liu, P.; Hao, J. W.; Liang, S. J.; Liang, G. L.; Wang, J. Y.; Zhang, Z. H. Choline chloride and itaconic acid-based deep eutectic solvent as an efficient and reusable medium for the preparation of 13-aryl-5H-dibenzo [b, i] xanthene-5, 7, 12, 14 (13H)-tetraones. *Monatsh. Chem.* **2016**, *147*, 801−808.
(33) Adeyemi, I.; Abu-Zahra, M. R.; Alnashef, I. Experimental study of the solubility of CO_2 in novel amine based deep eutectic solvents. *Energy Procedia* **2017**, *105*, 1394−1400.
(34) Liu, F.; Huang, K.; Jiang, L. Promoted adsorption of CO_2 on amine-impregnated adsorbents by functionalized ionic liquids. *AIChE J.* **2018**, *64*, 3671−3679.
(35) Peng, H. L.; Zhang, J. B.; Zhang, J. Y.; Zhong, F. Y.; Wu, P. K.; Huang, K.; Fan, J. P.; Liu, F. Chitosan-Derived Mesoporous Carbon with Ultrahigh Pore Volume for Amine Impregnation and Highly Efficient CO_2 Capture. *Chem. Eng. J.* **2019**, *359*, 1159−1165.
(36) Chen, F. F.; Huang, K.; Fan, J. P.; Tao, D. J. Chemical solvent in chemical solvent: A class of hybrid materials for effective capture of CO_2. *AIChE J.* **2018**, *64*, 632−639.
(37) Liu, X.; Ao, Q.; Shi, S.; Li, S. CO_2 capture by alcohol ammonia based deep eutectic solvents with different water content. *Mater. Res. Express* **2022**, *9*, 2−8.
(38) Ren, H.; Lian, S.; Wang, X.; Zhang, Y.; Duan, E. Exploiting the hydrophilic role of natural deep eutectic solvents for greening CO_2 capture. *J. Cleaner Prod.* **2018**, *193*, 802−810.
(39) Trivedi, T. J.; Lee, J. H.; Lee, H. J.; Jeong, Y. K.; Choi, J. W. Deep eutectic solvents as attractive media for CO_2 capture. *Green Chem.* **2016**, *18*, 2834−2842.
(40) Yan, H.; Zhao, L.; Bai, Y.; Li, F.; Dong, H.; Wang, H.; Zhang, X.; Zeng, S. Superbase ionic liquid-based deep eutectic solvents for improving CO_2 absorption. *ACS Sustainable Chem. Eng.* **2020**, *8*, 2523−2530.
(41) Saravanamurugan, S.; Kunov-Kruse, A. J.; Fehrmann, R.; Riisager, A. Amine-Functionalized Amino Acid-based Ionic Liquids as Efficient and High-Capacity Absorbents for CO_2. *ChemSusChem* **2014**, *7*, 897−902.
(42) Gurkan, B. E.; de la Fuente, J. C.; Mindrup, E. M.; Ficke, L. E.; Goodrich, B. F.; Price, E. A.; Schneider, W. F.; Brennecke, J. F. Equimolar CO_2 Absorption by Anion-Functionalized Ionic Liquids. *J. Am. Chem. Soc.* **2010**, *132*, 2116−2117.
(43) Zhang, K.; Hou, Y.; Wang, Y.; Wang, K.; Ren, S.; Wu, W. Efficient and Reversible Absorption of CO_2 by Functional Deep Eutectic Solvents. *Energy Fuels* **2018**, *32*, 7727−7733.
(44) Sarmad, S.; Mikkola, J. P.; Ji, X. Carbon dioxide capture with ionic liquids and deep eutectic solvents: a new generation of sorbents. *ChemSusChem* **2017**, *10*, 324−352.

https://doi.org/10.1021/acsomega.2c06437
ACS Omega 2022, 7, 48272−48281